Horizontal gene transfer and shifts in linked bacterial community composition are associated with maintenance of antibiotic resistance genes during food waste composting

Authors: Hanpeng Liao[1], Ville-Petri Friman[2], Stefan Geisen[3], Qian Zhao[1], Peng Cui[1], Xiaomei Lu[1], Zhi Chen[1], Zhen Yu[4], Shungui Zhou[*1]

Author affiliation:

[1] Fujian Provincial Key Laboratory of Soil Environmental Health and Regulation, College of Resources and Environment, Fuzhou 350002, China;

[2] Department of Biology, Wentworth Way, YO10 5DD, University of York, York, UK;

[3] Department of Terrestrial Ecology, Netherlands Institute of Ecology, Wageningen, Netherlands;

[4] Guangdong Key Laboratory of Integrated Agro-environmental Pollution Control and Management, Guangdong Institute of Eco-environmental Science & Technology, Guangzhou 510650, China;

* Corresponding author: Prof. Shungui Zhou

Email: sgzhou@soil.gd.cn, Phone: +86-590-86398509, Fax: +86-590-86398509.

Horizontal gene transfer and shifts in linked bacterial community composition are associated with maintenance of antibiotic resistance genes during food waste composting

Abstract

About 1.3 billion tons of food waste (FW) is annually produced at a global scale. A major fraction of FW is deposited into landfills thereby contributing to environmental pollution and emission of greenhouse gasses. While increasing amounts of FW are recycled more sustainably into fertilizers in industrial-scale composting, very little is known about the antibiotic resistance genes (ARGs) present in FW and how their abundance is affected by composting. To study this, we quantified the diversity and abundance of ARGs, mobile genetic elements (MGEs) and bacterial communities in the beginning, during and at the end of the FW composting. All targeted 27 ARGs and 5 MGEs were detected in every sample suggesting that composted FW remains a reservoir of ARGs and MGEs. While the composting drastically changed the abundance, composition and diversity of bacterial communities, an increase in total ARG and MGE abundances was observed. Changes in ARGs were linked with shifts in the composition of bacterial communities as revealed by a Procrustes analysis ($P < 0.01$). Crucially, even though the high composting temperatures reduced the abundance and diversity of initially ARG-associated bacterial taxa, ARG abundances were maintained in other associated bacterial taxa. This was likely driven by horizontal gene transfer and physicochemical composting properties as revealed by a clear positive correlation between ARGs, MGEs, pH, NO_3^- and moisture. Together our findings suggest that traditional composting is not efficient at removing ARGs and MGEs from FW. More effective composting strategies are thus needed to

minimize ARG release from composted FW into agricultural environments.

Keywords: Antibiotic resistance genes, Municipal solid waste, Mobile genetic elements, Bacterial community composition, Composting physicochemical parameters

1. Introduction

A significant portion of food ends up as unused waste resulting in more than 1.3 billion tons of food waste (FW) annually at the global scale (Gustavsson et al., 2011). In China and in the U.S. about 90% of FW ends up in landfills (Breunig et al., 2017; Yong et al., 2015). However, landfilling FW is unsustainable leading to increased greenhouse gas emissions and prevents the required land from being used for other purposes (Zhang et al., 2014). Composting FW into organic fertilizers provides an environmentally friendly alternative to FW landfilling and is increasingly used around the world (Cerda et al., 2018; Li et al., 2013; Wang et al., 2017b). However, there exists only little information about composting of FW. One potential risk could be human-associated pathogens and bacteria-associated antibiotic resistance genes that could potentially get enriched during the composting process (ADD REF). Antibiotic resistance is recognized as a major threat to public health worldwide and antibiotic resistant bacteria and antibiotic resistance genes (ARGs) are widely found in the natural environments, wastewater, manure, and sewage sludge (Lekunberri et al., 2017; Ma et al., 2015; Su et al., 2017b). Previous studies have shown that ARGs are found in various foods such as pork, beef, raw fruits and fresh vegetables (Rolain, 2013; Ruimy et al., 2010). However, the identity and composition of ARGs and MGEs in FW remains unknown. Many antibiotic-resistant microbes, including both foodborne pathogenic and commensal bacteria, are also found in food chains ranging

from manufacturing to commercial products (Wang et al., 2012) and numerous studies support the link between the use of antibiotics and enrichment of ARGs during agricultural production. Food waste could thus serve as an important source of ARGs and MGEs similar to other types of organic wastes such as sewage sludge (Su et al., 2017a) and animal manure (Wang et al., 2017a). Hence, it is important to understand how FW composting impacts the abundance, mobility and diversity of ARGs to minimize the potential spread of ARGs to agricultural environments along the final composting products.

Agricultural application of composted organic waste introduces high loads of bacteria that often carry ARGs into the soil (Xie et al., 2016). In the soil, ARGs propagate along with their bacterial hosts and can disseminate via horizontal gene transfer between different bacterial species, including many human pathogenic bacteria (Forsberg et al., 2014). Mobile genetic elements (MGEs), such as plasmids, integrons and transposons are often linked with ARGs and their horizontal dissemination (Bengtsson-Palme et al., 2018; Gillings, 2017) and they often confer resistance to multiple antibiotics (Pehrsson et al., 2016). If ARGs enter humans via the food chain, the efficiency of antibiotics could be reduced. While the diversity and abundance of ARGs and MGEs has been studied largely in the process of manure and sewage sludge composting (Ma et al., 2015; Su et al., 2017b; Wu et al., 2017), there are no studies investigating ARG and MGE dynamics during FW composting. Even though most food products do not normally contain antibiotics, the emergence of abundant ARGs have been found in some food products such as meat and dairy products (Wang et al., 2012). It is thus important to understand the abundance and distribution of ARGs and MGEs in FW, if these genes are mobile or associated with certain bacterial hosts, and crucially, whether composting can be used to remove or

considerably reduce their abundance resulting in safe composting end product (Liao et al., 2018).

FW has many specific physical and chemical characteristics that separates it from other organic wastes including high organic matter content, high salt, oil and protein content and low pH (Cerda et al., 2018). It is known that these properties have a strong effect for the transmission of ARGs (Bengtsson-Palme et al., 2018). For example, Liu *et al.* found that salinity can improve the removal of antibiotic resistance genes in wastewater treatment bioreactors (Liu et al., 2018). However, it is unclear how the specific physicochemical properties of FW affect the dynamics of ARGs during composting. Composting is a complex fermentation process that induces dynamic changes in biotic components such as the microbial community structure and abiotic factors including physicochemical properties of compost (Su et al., 2015; Zhang et al., 2016). These could potentially drive the abundance and composition of ARGs and MGEs directly or have indirect effects on their bacterial hosts. For example, composting temperature has been shown to play an important role in removing ARGs via effects on MGEs and on the bacterial community composition (Liao et al., 2018).

Here we investigated the impact of FW composting on the abundance of ARGs, MGEs and soil bacterial community composition, diversity and densities at an industrial scale. The objectives of our study were: (1) to investigate the abundance and diversity of ARGs and MGEs during FW composting; (2) to determine potential bacterial carriers of ARGs and MGEs (3) to understand the relative importance of various biotic and abiotic factors (composting properties, bacterial community diversity, bacterial community composition and MGE abundances) on the dynamics and abundance of ARGs during FW composting. To this end, we used temporal

sampling followed by quantitative PCR (qPCR) to determine the abundances of 27 ARGs and 5 MGEs in a full-scale FW composting experiment. Furthermore, we applied Illumina Hiseq sequencing of the bacterial 16S rRNA genes to determine the composition of the ARG and MGE-associated bacterial communities.

2. Materials and methods

2.1 Full-scale experimental setup for food waste composting

FW composting experiments were conducted in a full-scale aerobic composting plant located in Jinshui district, Zhengzhou, China. The aerobic composting process has previously been described by Liao et al. (2018) and the same methods were used in this experiment with some modifications. Briefly, raw composting materials consisted of deoiled FW (with 78% water content, provided by Xinmi food waste processing factory) and tobacco powder (with 20% water content, provided by Zhengzhou cigarette factory). Tobacco powder was used as a composting amendment as it is an abundant and accessible waste produced locally near the composting plant. Approximately 80 tons of composting material was created by mixing FW and tobacco powder in a ratio of 3:1 (v/v), respectively. The final composting material had approximately 58% water content. The composting mixture was loaded into three independent replicate piles (8 m length, 6 m width, and 3 m height) at 2.2 m bulk height. Forced aeration was supplied from the bottom to the top of the pile according to aeration needs during different phases of composting (Liao et al., 2018). To mix the compost substrate well and to reduce pile-edge effects, mechanical turning of the composting material was performed every seven days using pile-specific forklifts to prevent cross-contamination between replicate piles.

2.2 Sample collection and DNA extraction

Samples were collected at 0, 5, 10, 13, 24, 30, 41, and 50 days after start of the composting, which allowed us to follow changes during various temperature stages during the composting process. The sampling process followed a previously described protocol by Liao et al. (2018) with some minor modifications. Briefly, to obtain representative samples at each sampling time point, each pile was diagonally divided into five domains, and each domain was sub-sampled (5000 g) from three different depths from the top of the pile: 40-50 cm (top), 90-100 cm (middle) and 150-160 cm (bottom). All sub-samples per sampled domain were pooled to obtain a final sample (5 samples per replicate pile totaling 15 total samples per sampling time point), homogenized and further divided into two 400 g aliquots of which one was stored in liquid nitrogen for biological analyses and the other one was stored at 4 °C for physicochemical analyses. This sampling approach was chosen to reduce the potential bias caused by the heterogeneity of the original composting substrate in each replicate pile. The ALFA-SEQ Advanced Soil Kit (mCHIP, Guangzhou, China) was used to extract genomic DNA from freeze-dried samples (200 mg) according to the manufacturer's instructions. DNA extraction was conducted three times per sample and purified DNA samples were pooled for sequencing and genetic analysis. The quality of DNA was quantified with NanoDrop ND-2000 (Thermo Fisher Scientific, Wilmington, USA) spectrophotometric analysis and visualized on a 1% agarose gel and normalized to equal concentrations before downstream qPCR processing.

2.3 Determination of physicochemical parameters during composting

We used previously described methods (Liao et al., 2018) to measure physicochemical properties during the composting: pH, temperature (Temp), water content (WC), total nitrogen content (TN), total carbon content (TC), total organic

carbon content (TOC), oil content (OIC), inorganic carbon content (IC) and ammonium (NH_4^+), sodium (NC) and nitrate (NO_3^-) concentrations. Briefly, TOC and IC were measured using an automatic TOC analyzer for liquid samples (Shimadzu TOC-L CPH, Kyoto, Japan). TN and TC were determined in an Elementar instrument (Vario MAX cube, Hanau, Germany) using dry combustion. OIC was measured using Soxhlet extractor method as described previously (Wang et al., 2017b). NC analysis was carried out with flame spectrophotometry. EC and pH were determined using a conductivity meter (Radiometer, model CDM210) and a pH meter (PB-10, Sartorius, Germany), respectively. NH_4^+ and NO_3^- were measured by a continuous-flow autoanalyser (FlowSys, Systea, Rome, Italy). WC was determined as the weight loss upon drying in an oven at 105 °C for 24 h. Daily monitoring of the composting temperature was measured with automatic thermometers placed at different depths of composting piles.

2.4 Measuring changes in ARG and MGE abundances with quantitative PCR (qPCR)

It has previously been shown that tetracycline, macrolide, aminoglycoside and sulfonamide resistance genes are the most common ARGs in organic waste (Su et al., 2015; Wang et al., 2017a). Therefore, we decided to study the abundance of these ARGs during FW composting by choosing ten tetracycline resistance genes (*tetA*, *tetB*, *tetC*, *tetG*, *tetL*, *tetM*, *tetQ*, *tetO*, *tetW*, and *tetX*), seven macrolide resistance genes (*ermB*, *ermF*, *ermM, ermT*, *ermX*, *mefA*, and *ereA*), seven aminoglycoside resistance genes (*aacA4*, *aadA*, *aadB*, *aadE*, *aphA1*, *strA*, and *strB*), and three sulfonamide resistance genes (*sul1*, *sul2*, and *sul3*) totaling 27 different ARGs. To investigate potential changes in the abundance of mobile genetic elements (MGEs), we measured

abundances of two integrase genes (*intI1*, *intI2*), two plasmid genes (*ISCR1*, *IncQ*) and one transposon (*Tn916/1545*, abbreviated as *Tn916*) gene that have often been connected with the movement of ARGs in the environment (Ma et al., 2017; Zhang et al., 2016). The bacterial abundance was measured as 16S rRNA gene copy numbers using SYBR-Green qPCR. All information about primers, annealing temperatures and amplification sizes used for all target genes are listed in Table S1. The qPCR reactions were carried out in a LightCycler 96 System (Roche, Mannheim, Germany) using 96-well plates. After amplification, a melting curve analysis with a temperature gradient ranging from 0.1 °C/s to 70 °C and to 95 °C was performed to confirm that only specific products were amplified. Standards were created using plasmids carrying target genes with TA cloning and extracted using a TIAN pure Mini Plasmid kit (Tiangen, Beijing, China). Concentrations of the standard plasmids (ng/μL) were determined using Nanodrop ND-2000 (Thermo Fisher Scientific, Wilmington, USA) to calculate copy number concentrations (copies/mL). Each qPCR reaction contained 10 μL GoTaq qPCR Master Mix (Promega, Madison, USA), 1.5 μL of each forward and reverse primers (4 mmol/L), 1 μL of template genomic DNA (approximately 10 ng), and 6 μL of nuclease-free water. Amplification conditions were 95 °C for 2 min, followed by 40 cycles of denaturation at 95 °C for 30s per cycle, annealing for 30 to 45s according to the amplicon length at the primer-specific annealing temperature (detail in Table S1), and extension for 30s at 72 °C. The amplification efficiencies of all qPCR products ranged from 90% to 110% with linear coefficient (R^2) values above 0.99 for all standard curves. Each reaction was run in triplicate alongside negative controls including DNA-free water instead of template genomic DNA. Absolute abundances of target genes are presented as gene copy numbers per gram of dry compost sample, while the relative abundances of target genes are shown as target

genes per 16S rRNA gene copy numbers.

2.5 Sequencing and bioinformatic analyses of the bacterial community composition during composting

We used 16S rRNA amplicon sequencing to determine changes in bacterial community diversity and composition during composting. The V4 region of the bacterial 16S rRNA gene was amplified using 515F (GTGCCAGCMGCCGCGGTAA)/806R (GGACTACHVGGGTWTCTAAT) primers and sequenced with the Illumina Hiseq 2500 platform and paired-end sequencing (2 × 150 bp) (Biddle et al., 2008). DNA libraries were prepared with an Illumina Hiseq Nextera library preparation kit following the manufacturer's protocol. The reverse primer contained a unique barcode for each sample and DNA was amplified in triplicate before sequencing. The amplification was initiated at 94 °C for 5 min and followed by 31 amplification rounds (94 °C for 30s, 52 °C for 30s, 72 °C for 45s and 72 °C for 10 min). Raw Illumina sequence data was processed with a pipeline coupling Trimmomatic (v 0.33) and QIIME (v 1.9.1) (Caporaso et al., 2010). Briefly, the raw sequences with low-quality reads that contained ambiguous nucleotides, mismatches in primer regions, or a length shorter than 100 bp were removed (An et al., 2018). Sequences were clustered into operational taxonomic units (OTUs) with UCLUST (version) at 97% sequence similarity (Edgar, 2010). Taxonomic OTU assignment was performed up to an 80% threshold using a Ribosome Database Project Classifier as described previously using the Greengenes database (McDonald et al., 2012). The normalization of the quality-curated sequences was conducted by subsampling to 10,759 sequences from each sample data set. Alpha-diversity was estimated using OTU richness based on the number of OTUs, phylogenetic diversity,

Dominance, Chao1, Shannon and Simpson diversity indices. Differences between microbial communities (beta-diversity) and principal coordinate analysis (PCoA) were analyzed based on the weighted Unifrac distances. All sequences were deposited in the National Center for Biotechnology Information Sequence Read Archive under the accession number SRP156265.

2.6 Analyzing and visualizing bacterial, ARG and MGE co-occurrence networks

Co-occurrence network analysis was used to explore pairwise correlations between bacterial taxa and different ARGs and MGEs during FW composting. Several previous reports have demonstrated that the non-random co-occurrence patterns could provide indirect evidence for potential host bacteria of ARGs and MGEs (Liao et al., 2018; Su et al., 2017b). Pairwise correlations were determined using Pearson and Spearman correlations as described previously (Hu et al., 2017). Only relatively large correlation coefficients ($\rho > 0.8$ and $P < 0.01$) detected with both methods (Pearson and Spearman) were included into network analyses to minimize false-positive correlations. Furthermore, the Benjamini-Hochberg procedure (q-value, $q < 0.01$) was performed to adjust *P*-values of all correlations to control false-discovery rate. The remaining significant interactions between ARGs, MGEs and bacteria were visualized as a network in Cytoscape v3.4.0, and network statistics were analyzed with Network Analyzer as undirected networks using default settings (Cline et al., 2007).

2.7 Statistical analyses

Data were analyzed using repeated measures ANOVA (ARG and MGE density dynamics), PCoA, redundancy analysis (RDA), PERMANOVA test, and Procrustes test for correlation analysis between ARGs and bacterial community composition with

the vegan package v2.4-3 in R 3.3.2. Heat maps represent log-transformed relative abundances of ARGs and MGEs and were drawn with *ggplot2* package in R 3.3.2. Linear Discriminant Analysis Effect Size analysis (LEfSe) was used to determine differentially abundant taxa between different stages of composting following methods by Segata et al. (2011). Finally, a partial least squares path modeling (PLS-PM) was used to explore relationships between physicochemical composting properties (Temp, WC, pH, IC, TN, TC, TOC, NH_4^+, NO_3^-, OC, and NC), bacterial alpha-diversity (based on OTU numbers, phylogenetic diversity, Dominance, Chao1, Shannon and Simpson diversity indices), bacterial community composition (based on relative OTU abundances), MGEs (relative abundances), and ARGs (relative abundances). PLS-PM is a powerful statistical method to study interactive relationships among observed and latent variables (Wagg et al., 2014) and is widely applied to explain and predict relationships in multivariate data sets (Puech et al., 2015). Path coefficients (i.e. standardized partial regression coefficients) represent the direction and strength of the linear relationships between variables (direct effects). Indirect effects are the multiplied path coefficients between a predictor and a response variable, adding the product of all possible paths excluding the direct effect. Models with different structures were evaluated using the Goodness of Fit (GoF) statistic, a measure of their overall predictive power. The R package plspm (v 0.4.7) was used to construct the final PLS-PM model.

3. Results and Discussion

3.1 Tracing ARG and MGE abundances and diversity throughout composting

The total concentrations of ARGs and MGEs in the initial raw FW were approximately 1.5×10^{10} and 2.0×10^{9} gene copies per gram (dry weight) of FW,

276 respectively (Figure S1). In contrast, the initial tobacco powder contained very low
277 amounts of ARGs (0.45% of ARGs observed in FW) and was not thus included in our
278 analysis of initial ARG and MGE composition. The tetracycline and macrolide
279 resistance genes were the most dominant genes accounting for 84.3% of total ARGs
280 while the transposon *Tn916* gene was the most dominant MGE in the initial FW
281 accounting for 94.2% of all MGEs (Figure S1). We also detected all targeted 27
282 ARGs and 5 MGEs that were initially present in the FW samples in the end of the
283 composting (Figure S2). Surprisingly, the total abundances of all ARGs and MGEs
284 significantly increased during the 50 days of FW composting ($P < 0.01$, Figure 1a). In
285 particular, the abundances of *tetL*, *sul2*, *strA*, *ermB*, *ISCR1* and *intI1* were enriched by
286 9.5, 10.7, 10.7, 377.2, 69.4, and 48.0 times, respectively (Figure 1c). This result is in
287 line with previous studies showing that abundances of *tetL*, *sul2*, *ermB* can be found
288 in reasonably high abundances after composting (Qian et al., 2016; Zhang et al., 2016).
289 One explanation could be that these ARGs were located in bacteria that were tolerant
290 to high temperatures. Alternatively, ARGs could have been located in MGEs that
291 could have been able to relocate to thermophilic bacteria during composting. We
292 found support for the both hypotheses in terms of predictable changes in bacterial
293 community composition and positive correlation between the abundances of plasmid
294 (*ISCR1*) and mobile integron (*intI1*) genes with the increase in ARGs during
295 composting (Figure S3, $P < 0.001$). Together these results suggest that traditional
296 composting is not efficient enough to remove ARGs and MGEs from FW
297 (mechanisms discussed in more detail later). Instead, we observed that FW contained
298 a wide diversity and abundance of ARGs and MGEs that even increased during
299 composting. Our results thus suggest that FW could be an important but often
300 neglected source of ARGs which could also potentially serve as a transfer route for

ARGs between agricultural environments, food manufacturing processes and consumers (Berendonk et al., 2015; Verraes et al., 2013; Wang et al., 2012). Great caution should thus be taken in using FW as composting raw material. However, we also want to note that only one type of FW was investigated in this study, and hence, other FW types should be examined in future studies to explore the generality of our results.

To investigate the dynamics of ARGs during composting, we focused on the link between the abundances of bacteria, ARGs and MGEs during composting in more detail. We found that total bacterial abundances based on 16S rRNA gene copy numbers increased during composting (Figure 1a). This is in line with previous results (Wang et al., 2017b) and can be explained by the increased amount of nutrients that become available for microbial growth during composting (Adhikari et al., 2009). Crucially, the increase in the total bacteria abundances was relatively higher than the increase in ARGs, and as a result, the relative abundance of ARGs per number of bacterial cells decreased during the composting (Figure 1b and d, $P < 0.01$). Particularly, tetracycline, macrolide, aminoglycoside and sulfonamide resistance genes showed clear decreases in their relative abundance, while a significant but less drastic decrease in the relative abundance of MGEs was observed (Figure 1b and d, $P < 0.01$). Together, these results suggest that even though the absolute abundances of ARGs and MGEs increased during composting, their relative abundances decreased and fewer bacteria carried ARGs and MGEs at the end of composting. This could have been due to because composting conditions favored non-ARG carrying bacteria, because carrying ARGs incurred fitness costs reducing bacterial competitive ability (Durão et al., 2018) or because bacteria that were less susceptible to MGEs became more abundant (Youngquist et al., 2016). While all these hypotheses should be tested

in the future experiments to better understand the mobilization of ARGs during composting, our study suggest that concentrating both absolute and relative ARG abundances is important for predicting the risk of ARG movement across different environmental compartments.

Figure 1

3.2 Changes in the bacterial community composition during FW composting

The composting process significantly influenced the composition of bacterial communities as shown in the non-metric multidimensional scaling plot based on weighted Unifrac distances (PERMANOVA test, R^2=0.8571, $P < 0.01$, Figure 2a). The bacterial community composition showed also a distinct clustering at different phases of composting based on Unweighted Pair-group Method with Arithmetic Mean (UPGMA) clustering (Figure S4). This result was further confirmed in a PCoA based on the weighted UniFrac distances (Figure S5) and LEfSe (Figure S6). These results are similar to previous studies and demonstrate that distinct changes in the bacterial community occur throughout composting (Su et al., 2015; Zainudin et al., 2017) and this is probably due to changes in temperature, physicochemical composting properties and a natural succession of microbial communities. Alpha-diversity of the bacterial community varied significantly during composting (Table S2). In particular, OTU richness slightly increased until 24 days then decreased significantly compared to the initial FW (Figure 2b, $P < 0.01$). This was likely due to a removal of thermolabile bacteria by the high composting temperature (approximately 65 °C) and an increased abundance of thermotolerant bacteria. In support of this, the composition of bacterial communities measured at the phylum level displayed clear temporal

dynamics during 50 days of composting (Figure 2c). More specifically, the relative abundance of Acidobacteria, Proteobacteria, and Bacteroidetes decreased from 21.59% to 7.12%, from 7.70% to 0.57%, and from 2.46% to 0.024%, respectively. Correspondingly, Firmicutes (principally consisting of the family Staphylococcaceae and Bacillaceae) increased from 67.95% to 91.90%. The majority of Bacillaceae form heat-resistant spores that provide a competitive advantage over thermolabile bacteria at elevated temperatures during composting (Liao et al., 2018; Zhang et al., 2015). Interestingly, the increase in Staphylococcaceae abundance from 0.8% to 22.0% towards the end of composting correlated positively with the increase in total ARG and MGE abundances (Figure S7, $P < 0.01$). Staphylococcaceae includes several food-related, often antibiotic resistant pathogens that often naturally carry various ARGs and MGEs (Ravcheev and Rodionov, 2011). Specifically, the foodborne bacterial genera *Jeotgalicoccus* and *Staphylococcus* (Deák, 2011) (both within Staphylococcaceae) increased in abundance during composting and replaced various initially dominant genera in the FW: *Bacillus* (22.43%), *Oceanobacillus* (21.95%), and *Corynebacterium* (12.92%) (Figures 2d and Figure S8). It has been shown previously that incubation at 80 °C for 60 min is required to completely kill *Staphylococcus aureus* (Yang et al., 2008). Therefore, it is likely that the maximum temperature of 65 °C was not high enough to eradicate these bacteria. This is in line with previous studies showing that most foodborne pathogens such as *Staphylococcus* spp. and *Enterococcus* spp. persist during composting (Awasthi et al., 2018). Together, these results suggest that composting can predictably change the composition of bacterial communities potentially favouring bacteria that can resist periodically high temperatures, and hence, be also responsible for carrying and disseminating ARGs and MGEs during FW composting.

Figure 2

3.3 Relationships between ARGs and MGEs with different taxa in bacterial communities

A Procrustes analysis based on bacterial OTUs and ARG abundances showed that ARGs significantly correlated with the bacterial community composition (Figure S9, M^2= 0.5675, R = 0.7407, $P < 0.0001$, 9999 permutations). Similarly, the relative and total MGE abundances correlated positively with total ARG abundances ($P < 0.001$, Figure S10a) and this finding was further confirmed by nonrandom co-occurrence patterns between individual ARGs and MGEs (Table 1 and Figure S10b). These results indicate that MGEs likely played an important role in the dissemination of ARGs during FW composting, which is consistent with previous findings on ARG movement in general (Bengtsson-Palme et al., 2018; Gillings, 2017; Zhu et al., 2017). The relationships between individual ARGs, MGEs and abundances of different bacterial taxa were further explored using correlation-based network analyses. We found that most ARGs and MGEs (87%) correlated positively ($P < 0.01$) with 18 bacterial genera. All these ARG-associated genera belonged to four phyla: Firmicutes, Acidobacteria, Proteobacteria, and Bacteroidetes (Figure 3a). Consistent with previous finding (Liao et al., 2018), more than 65% of ARG- and MGE-associated bacteria belonged to Proteobacteria and Firmicutes (Figure S11), which were the dominant phyla in the initial FW material. Together these results further suggest that MGEs and ARGs are strongly linked with certain bacterial taxa in FW.

Many bacteria frequently carry multiple ARGs and/or MGEs at the same time in their plasmids, which are considered as the main vehicle for horizontal transfer of

401 genetic material (Zhang et al., 2011). In support of this, we found that for example the
402 genus *Acinetobacter* was significantly associated with 22 different resistance genes,
403 while *Sphingobacterium* and *Lactobacillus* had significant associations with 20 and 9
404 different resistance genes, respectively. Certain *Acinetobacter* spp. are
405 multidrug-resistant and act as major infection agents in debilitated patients (Towner,
406 2009). Similarly, *Lactococcus lactis* has been shown to carry genes conferring
407 resistance to tetracycline, erythromycin, and vancomycin (Mathur and Singh, 2005).
408 We also found that *Acinetobacter*, *Alcaligenes*, and *Ignatzschineria* correlated with
409 three MGEs (*IncQ*, *intI2*, and *Tn916*) and multiple ARGs (Figure S12), suggesting
410 that these bacterial genera might act as hubs for horizontal transfer of ARGs. Our
411 results thus suggest that ARGs could have been maintained as multi-drug resistance
412 plasmids or transposons in bacterial community and be potentially transferred by a
413 certain key group of bacteria. However, we have to note that our DNA-based
414 approach cannot fully address whether microorganisms were viable. Therefore,
415 cultivation-based approaches are needed to confirm that ARG-carrying
416 microorganisms in the compost are active. Furthermore, subsequent genome
417 sequencing would allow to detect the exact number and diversity of ARGs within
418 individual species and if ARGs are located in the bacterial chromosome or plasmids.

419 We next explored the dynamics of ARG and/or MGE-associated bacteria during
420 composting. In the initial FW material, *Bacillus* (22.4%), *Oceanobacillus* (21.9%),
421 *Corynebacterium* (12.9%), *Saccharomonospora* (6.8%), and *Ignatzschineria* (5.7%)
422 were the main ARG/MGE-associated bacteria (67.0% of total 16S rRNA gene
423 sequences). The abundance of these genera gradually decreased to 23.3% during 50
424 days of composting (Figure 3b), and at the same time, the relative abundance of the
425 genera (*Jeotgalicoccus*, *Staphylococcus*, and *Sporosarcina*) increased by 123.9, 11.6,

and 6.3 times, respectively. This gives more support to the idea that ARG and MGE-associated taxa increased during the composting likely due to the high composting temperature (Burch et al., 2017; Su et al., 2015). Although the maximum temperature during composting reached up to 65 °C (>55 °C for approximately 7 days, Figure S13), most bacterial genera still persisted and some genera even increased in their relative abundance over time (Figure 3b). While this shift could have been driven by horizontal gene transfer between heat-susceptible and tolerant bacteria in the beginning of the experiment, it is also possible that ARGs and MGEs survived at elevated composting temperatures as a cell-free DNA and were picked up by other bacteria later during composting. For example, a previous laboratory study has shown that cell-free DNA is stable even at temperatures up to 70 °C (Zhang and Wu, 2005) and that cell-free DNA or plasmids originating from lysed bacterial cells at high temperature can contain ARGs and/or MGEs (Nielsen et al., 2007). Together these results suggest that FW contains several bacterial taxa that may disseminate ARGs to other bacterial hosts through horizontal gene transfer and due to their survival at high temperatures. In addition to plasmids, alternative carriers of ARGs or MGEs, such as bacteriophages (Lekunberri et al., 2017; Wang et al., 2018), which were not investigated here, should be included in future studies.

Figure 3

Table 1

3.4 Determining the relative importance of bacterial community composition and diversity, MGEs and physicochemical properties for ARG abundances during composting

The results from the RDA analysis showed that selected variables (including physicochemical composting properties, bacterial community composition and MGE abundances) could explain 74% of the total variance of ARG abundance dynamics during composting (Figure S14). To further study how ARGs were affected by biotic and abiotic factors during composting, we built a Partial Least Squares Path Model (PLS-PM) describing direct and indirect relationships between different variables. We found that both physicochemical composting properties and MGE abundances had equally strong direct positive effects on ARG abundances, while bacterial community diversity or composition had no statistically significant effect (Figure 4). This result is in contrast with a previous finding showing that the bacterial community composition is the main factor driving changes in ARG abundances in a mariculture sediment (Han et al., 2017). However, it is consistent with another study, where environmental factors rather than bacterial community composition were more important in driving changes in ARG abundances during composting (Liao et al., 2018). Composting properties also had direct positive effects on bacterial community composition and alpha-diversity, and indirect positive effects on MGE abundances via bacterial community composition. MGEs have recently been proposed to have a more important role in the spread of ARGs than the microbial community composition or microbial diversity (Ma et al., 2017; Wu et al., 2017). One possible reason may be that MGEs are very successful at mobilizing ARGs in environmental microbial communities via horizontal gene transfer (Wang et al., 2017a). Additionally, resistance genes are often clustered for example in multi-drug resistance plasmids. Together with the PLS-PM analysis (Figure 4b), our results provide more support to the idea that changes in ARG abundances were likely driven by horizontal gene transfer (MGEs), which itself was strongly affected by the bacterial community

composition. While previous research has connected the microbial community structure with predictable changes in ARG abundances in various environments (Su et al., 2015; Wu et al., 2017), our results suggest that also physicochemical composting properties can directly and indirectly change ARG abundances during FW composting. This could be specifically explained by certain properties, such as temperature and pH, that can have direct positive effects on ARG- and MGE-associated bacterial growth during composting (Awasthi et al., 2018). For example, high temperature will decompose polymeric substances present in the FW increasing nutrient availability (Li et al., 2013).

To better understand the specific composting properties influencing ARG abundances, we used variance partitioning to analyze our data in more detail (VPA). We found that pH, NO_3^- concentration and water content (WC) alone explained 9.1%, 12.9%, and 9.1% of total variation of ARG abundances, respectively (Figure 4c). Interestingly, interactive effects between pH and WC and pH, WC and NO_3^- explained 35.2 % and 12.6% of the total variation of ARG abundances, respectively (Figure 4c). The initially low pH (4.4) remained below 5.5 during the first 30 days of composting (Figure S13). This likely resulted from the acidification of FW that contained organic acids and some low-molecular-weight volatiles produced by microbes (Yu and Huang, 2009), which could have prevented the growth of indigenous bacteria (Awasthi et al., 2018) and constrained the horizontal transfer of ARGs via less frequent encounter rates during composting (Ma et al., 2015). In addition, moisture content played an important role alone and interactively with the pH. Moisture content is known to influence microbial activity, free airspace, temperature and aeration during composting (Awasthi et al., 2018) and could thus affect the connectivity and MGE-induced horizontal transfer of ARGs between

bacterial sub-populations. However, further work is needed to better understand how physicochemical properties and horizontal gene transfer might interactively drive ARG dynamics during composting.

Figure 4

4. Conclusions

Our study shows that FW is an important reservoir of ARGs and MGEs and that traditional composting is inefficient in removing the ARGs despite a clear decrease in relative abundances of ARGs. Moreover, our study supports the idea that horizontal gene transfer and physicochemical composting properties, such as temperature, pH and moisture, are important for disseminating and maintaining ARGs during FW composting. As a result, even though high composting temperatures reduced the number of initial ARG-associated bacterial taxa, ARGs were likely maintained in other bacterial taxa potentially due to horizontal gene transfer as indicated by strong positive correlations between ARGs and MGEs. These findings suggest that new composting methods are needed for removal of ARGs during composting to reduce the risk of disseminating ARGs to agricultural environments.

Acknowledgements

This work was supported by the National Key Research and Development Program of China (2017YFD0800203), National Natural Science Foundation of China (31601831), the National Key Technologies R&D Program of Fujian

(2017NZ0001-1). Fujian Agriculture and Forestry University Program for Distinguished Young Scholar (No. XJQ2017001). Ville-Petri Friman is supported by the Wellcome Trust [ref: 105624] through the Centre for Chronic Diseases and Disorders (C2D2) and Royal Society Research Grant (RSG\R1\180213) at the University of York. Stefan Geisen is supported by a NWO-VENI grant from the Netherlands Organization for Scientific Research (016.Veni.181.078). We would like to thank Beijing Geogreen lnnotech Co., Ltd for offering the experimental condition and Huan Liu for help in sampling.

Appendix A. Supplementary data

Supplementary data related to this article can be found online.

References

Adhikari BK, Barrington S, Martinez J, King S. Effectiveness of three bulking agents for food waste composting. Waste Manage. 2009; 29: 197-203.

An XL, Su JQ, Li B, Ouyang WY, Zhao Y, Chen QL, et al. Tracking antibiotic resistome during wastewater treatment using high throughput quantitative PCR. Environ. Int. 2018; 117: 146-153.

Awasthi SK, Wong JWC, Li J, Wang Q, Zhang Z, Kumar S, et al. Evaluation of microbial dynamics during post-consumption food waste composting. Bioresource. Technol. 2018; 251: 181-188.

Bengtsson-Palme J, Kristiansson E, Larsson DGJ. Environmental factors influencing the development and spread of antibiotic resistance. Fems Microbiol. Rev. 2018; 42: 68-80.

Berendonk TU, Manaia CM, Merlin C, Fatta-Kassinos D, Cytryn E, Walsh F, et al. Tackling antibiotic resistance: the environmental framework. Nat. Rev. Microbiol. 2015; 13: 310-317.

Biddle JF, Fitz-Gibbon S, Schuster SC, Brenchley JE, House CH. Metagenomic signatures of the Peru Margin subseafloor biosphere show a genetically distinct environment. Proc. Nat. Acad. Sci. U.S.A. 2008; 105: 10583-10588.

Breunig HM, Jin L, Robinson A, Scown CD. Bioenergy potential from food waste in California. Environ. Sci. Technol. 2017; 51: 1120-1128.

552 Burch T, Sadowsky MJ, LaPara TM. The effect of different treatment technologies on the fate of
553 antibiotic resistance genes and class 1 integrons when residual municipal wastewater solids are applied
554 to soil. Environ. Sci. Technol. 2017; 51: 14225–14232.
555 Caporaso JG, Kuczynski J, Stombaugh J, Bittinger K, Bushman FD, Costello EK, et al. QIIME allows
556 analysis of high-throughput community sequencing data. Nat. Methods 2010; 7: 335.
557 Cerda A, Artola A, Font X, Barrena R, Gea T, Sánchez A. Composting of food wastes: Status and
558 challenges. Bioresource. Technol. 2018; 248: 57-67.
559 Cline MS, Smoot M, Cerami E, Kuchinsky A, Landys N, Workman C, et al. Integration of biological
560 networks and gene expression data using Cytoscape. Nat. Protoc. 2007; 2: 2366.
561 Deák T. A survey of current taxonomy of common foodborne bacteria. Acta Aliment. Hung. 2011; 40:
562 95-116.
563 Durão P, Balbontín R, Gordo I. Evolutionary Mechanisms Shaping the Maintenance of Antibiotic
564 Resistance. Trends Microbiol. 2018; 26: 677-691.
565 Edgar RC. Search and clustering orders of magnitude faster than BLAST. Bioinformatics 2010; 26:
566 2460-2461.
567 Forsberg KJ, Patel S, Gibson MK, Lauber CL, Knight R, Fierer N, et al. Bacterial phylogeny structures
568 soil resistomes across habitats. Nature 2014; 509: 612.
569 Gillings MR. Class 1 integrons as invasive species. Curr. Opin. Biotech. 2017; 38: 10-15.
570 Gustavsson J, Cederberg C, Sonesson U, van Otterdijk R, Meybeck A. Global food losses and food
571 waste: extent, causes and prevention. FAO, Rome. Food and Agriculture Organization of the United
572 Nations 2011; http://www.fao.org/docrep/014/mb060e/mb060e00.pdf.
573 Han Y, Wang J, Zhao Z, Chen J, Lu H, Liu G. Fishmeal application induces antibiotic resistance gene
574 propagation in mariculture sediment. Environ. Sci. Technol. 2017; 51: 10850–10860.
575 Hu H, Wang J-T, Li J, Shi X, Ma Y, Chen D, et al. Long-term nickel contamination increases the
576 occurrence of antibiotic resistance genes in agricultural soils. Environ. Sci. Technol. 2017; 51: 790-800.
577 Lekunberri I, Villagrasa M, Balcázar JL, Borrego CM. Contribution of bacteriophage and plasmid DNA
578 to the mobilization of antibiotic resistance genes in a river receiving treated wastewater discharges. Sci.
579 Total. Environ. 2017; 601-602: 206-209.
580 Li Z, Lu H, Ren L, He L. Experimental and modeling approaches for food waste composting: A review.
581 Chemosphere 2013; 93: 1247-1257.

582 Liao H, Lu X, Rensing C, Friman VP, Geisen S, Chen Z, et al. Hyperthermophilic composting
583 accelerates the removal of antibiotic resistance genes and mobile genetic elements in sewage sludge.
584 Environ. Sci. Technol. 2018; 52: 266-276.
585 Liu M, Li Q, Sun H, Jia S, He X, Li M, et al. Impact of salinity on antibiotic resistance genes in
586 wastewater treatment bioreactors. Chem. Eng. J. 2018; 338: 557-563.
587 Ma L, Li A-d, Yin X-L, Zhang T. The prevalence of integrons as the carrier of antibiotic resistance
588 genes in natural and man-made environments. Environ. Sci. Technol. 2017; 51: 2720-5728.
589 Ma L, Xia Y, Li B, Yang Y, Li L-G, Tiedje JM, et al. Metagenomic assembly reveals hosts of antibiotic
590 resistance genes and the shared resistome in pig, chicken and human feces. Environ. Sci. Technol. 2015;
591 50: 420-427.
592 Mathur S, Singh R. Antibiotic resistance in food lactic acid bacteria—a review. Int. J. Food Microbiol
593 2005; 105: 281-295.
594 McDonald D, Price MN, Goodrich J, Nawrocki EP, DeSantis TZ, Probst A, et al. An improved
595 Greengenes taxonomy with explicit ranks for ecological and evolutionary analyses of bacteria and
596 archaea. ISME J 2012; 6: 610-618.
597 Nielsen KM, Johnsen PJ, Bensasson D, Daffonchio D. Release and persistence of extracellular DNA in
598 the environment. Environ. Biosaf. Res. 2007; 6: 37-53.
599 Pehrsson EC, Tsukayama P, Patel S, Mejía-Bautista M, Sosa-Soto G, Navarrete KM, et al.
600 Interconnected microbiomes and resistomes in low-income human habitats. Nature 2016; 533:
601 212-216.
602 Puech C, Poggi S, Baudry J, Aviron S. Do farming practices affect natural enemies at the landscape
603 scale? Landscape. Ecol. 2015; 30: 125-140.
604 Qian X, Sun W, Gu J, Wang X-J, Sun J-J, Yin Y-N, et al. Variable effects of oxytetracycline on
605 antibiotic resistance gene abundance and the bacterial community during aerobic composting of cow
606 manure. J. Hazard. Mater. 2016; 315: 61-69.
607 Ravcheev D, Rodionov D. Comparative genomics based reconstruction of transcription regulation
608 network in Staphylococcaceae. Moscow Conference on Computational Molecular Biology 2011; 305:
609 21-24.
610 Rolain JM. Food and human gut as reservoirs of transferable antibiotic resistance encoding genes.
611 Front. Microbiol. 2013; 4: 173.

612 Ruimy R, Brisabois A, Bernede C, Skurnik D, Barnat S, Arlet G, et al. Organic and conventional fruits
613 and vegetables contain equivalent counts of Gram-negative bacteria expressing resistance to
614 antibacterial agents. Environ. Microbiol. 2010; 12: 608-615.
615 Segata N, Izard J, Waldron L, Gevers D, Miropolsky L, Garrett WS, et al. Metagenomic biomarker
616 discovery and explanation. Genome. Biol. 2011; 12: R60.
617 Su J-Q, An X-L, Li B, Chen Q-L, Gillings MR, Chen H, et al. Metagenomics of urban sewage
618 identifies an extensively shared antibiotic resistome in China. Microbiome 2017a; 5: 84.
619 Su J-Q, Wei B, Ou-Yang W-Y, Huang F-Y, Zhao Y, Xu H-J, et al. Antibiotic resistome and its
620 association with bacterial communities during sewage sludge composting. Environ. Sci. Technol. 2015;
621 49: 7356-7363.
622 Su JQ, Cui L, Chen QL, An XL, Zhu YG. Application of genomic technologies to measure and monitor
623 antibiotic resistance in animals. Ann. Ny. Acad. Sci. 2017b; 1388: 121-135.
624 Towner KJ. Acinetobacter: an old friend, but a new enemy. J. Hosp. Infect. 2009; 73: 355-363.
625 Verraes C, Van Boxstael S, Van Meervenne E, Van Coillie E, Butaye P, Catry B, et al. Antimicrobial
626 resistance in the food chain: a review. Int. J. Env, Res, Pub, He, 2013; 10: 2643.
627 Wagg C, Bender SF, Widmer F, van der Heijden MG. Soil biodiversity and soil community
628 composition determine ecosystem multifunctionality. Proc. Nat. Acad. Sci. U.S.A. 2014; 111:
629 5266-5270.
630 Wang H, McEntire JC, Zhang L, Li X, Doyle M. The transfer of antibiotic resistance from food to
631 humans_ facts, implications and future directions. Rev. sci. tech. Off. int. Epiz 2012; 31: 249.
632 Wang H, Sangwan N, Li H-Y, Su J-Q, Oyang W-Y, Zhang Z-J, et al. The antibiotic resistome of swine
633 manure is significantly altered by association with the Musca domestica larvae gut microbiome. ISME.
634 J 2017a; 11: 100-111.
635 Wang M, Liu P, Zhou Q, Tao W, Sun Y, Zeng Z. Estimating the contribution of bacteriophage to the
636 dissemination of antibiotic resistance genes in pig feces. Environ. Pollut. 2018; 238: 291-298.
637 Wang X, Pan S, Zhang Z, Lin X, Zhang Y, Chen S. Effects of the feeding ratio of food waste on
638 fed-batch aerobic composting and its microbial community. Bioresource. Technol. 2017b; 224:
639 397-404.
640 Wu D, Huang X-H, Sun J-Z, Graham DW, Xie B. Antibiotic resistance genes and associated microbial
641 community conditions in aging landfill systems. Environ. Sci. Technol. 2017; 21: 12859–12867.

642 Xie W-Y, Mcgrath SP, Su J, Hirsch PR, Clark IM, Shen Q, et al. Long-term impact of field applications
643 of sewage sludge on soil antibiotic resistome. Environ. Sci. Technol. 2016; 50: 12602-12611.
644 Yang W, Zerbe H, Petzl W, Brunner RM, Günther J, Draing C, et al. Bovine TLR2 and TLR4 properly
645 transduce signals from Staphylococcus aureus and E. coli, but S. aureus fails to both activate NF-κB in
646 mammary epithelial cells and to quickly induce TNFα and interleukin-8 (CXCL8) expression in the
647 udder. Mol. Immunol. 2008; 45: 1385-1397.
648 Yong Z, Dong Y, Zhang X, Tan T. Anaerobic co-digestion of food waste and straw for biogas
649 production. Renew. Energ. 2015; 78: 527-530.
650 Youngquist CP, Mitchell SM, Cogger CG. Fate of antibiotics and antibiotic resistance during digestion
651 and composting: A review. J. Environ. Qual. 2016; 45: 537-545.
652 Yu H, Huang GH. Effects of sodium acetate as a pH control amendment on the composting of food
653 waste. Bioresource. Technol. 2009; 100: 2005-2011.
654 Zainudin MHM, Ramli N, Hassan MA, Shirai Y, Tashiro K, Sakai K, et al. Bacterial community shift
655 for monitoring the co-composting of oil palm empty fruit bunch and palm oil mill effluent anaerobic
656 sludge. J. Ind. Microbiol. Biot 2017; 44: 869-877.
657 Zhang C, Su H, Baeyens J, Tan T. Reviewing the anaerobic digestion of food waste for biogas
658 production. Renew. Sust. Energ. Rev. 2014; 38: 383-392.
659 Zhang J, Sui Q, Tong J, Buhe C, Wang R, Chen M, et al. Sludge bio-drying: Effective to reduce both
660 antibiotic resistance genes and mobile genetic elements. Water Res. 2016; 106: 62-70.
661 Zhang L, Ma H, Zhang H, Xun L, Chen G, Wang L. Thermomyces lanuginosus is the dominant fungus
662 in maize straw composts. Bioresource. Technol. 2015; 197: 266-275.
663 Zhang L, Wu Q. Single gene retrieval from thermally degraded DNA. J. Bioscience. 2005; 30:
664 599-604.
665 Zhang T, Zhang X-X, Ye L. Plasmid Metagenome Reveals High Levels of Antibiotic Resistance Genes
666 and Mobile Genetic Elements in Activated Sludge. PLOS ONE 2011; 6: e26041.
667 Zhu Y, Zhao Y, Li B, Huang C, Zhang S, Yu S, et al. Continental-scale pollution of estuaries with
668 antibiotic resistance genes. Nat. Microbiol. 2017; 2: 16270.
669
670

Figure captions

Figure 1. The dynamics of total ARG, MGE and bacterial abundances (16S rRNA gene copies) during FW composting. Panel (a-b): Changes in target gene (ARGs, MGEs and 16S rRNA) abundances during composting presented as the sum of target genes based on absolute (a) and relative gene abundances (b). Panel (c-d): Heat maps showing changes in the density of individual ARG and MGE gene abundances based on absolute (c) and relative abundance (d) during FW composting. Bars denote for mean ± standard error. Significance levels are indicated by * ($P < 0.05$), ** ($P < 0.01$) levels.

Figure 2. Changes in bacterial community composition and diversity during FW composting. Panel (a): Overall distribution pattern of OTU-based bacterial community dissimilarity during composting (non-metric multidimensional scaling (NMDS); ordination derived from weighted-UniFrac distances). Symbols with different colors denote for different sampling days. Panel (b): Changes in observed OTU number during composting. An asterisk (*) and two asterisks

(**) indicate significant differences at 0.05 and 0.01 significance levels, respectively. Panel (c): Relative abundance of different bacterial phyla during composting. (d): Ternary plot depicting the distribution of bacterial taxa (at genus level, relative abundance > 1%) at different stages of composting (D0 presents the control (day 0), D13 the thermophilic phase (day 13) and D50 the maturation phase (day 50))

Figure 3. Co-occurrence network showing positive associations between ARGs, MGEs and different bacterial taxa. Panel (a): Nodes coded with different colors and shapes represent different ARGs, MGEs and bacterial phyla, and the edges correspond to strong and significant correlations between nodes (P <0.01). Node sizes represent the relative abundances of ARGs, MGEs, and bacterial phyla during FW composting. Panel (b): Distribution profiles showing the relative abundance of ARG- and MGE-associated bacteria at genus level during FW composting. The legend on the right side of the panel denote for relative abundances (%) of total 16S rRNA gene sequences for each presented bacterial taxon.

Figure 4. Partial least squares path model (PLS-PM) showing direct and indirect effects of different factors on ARG abundances. Panel (a): PLS-PM describing the relationships between composting properties, bacterial diversity, bacterial community composition (at phylum level) and mobile genetic elements (MGEs) on ARG abundances. Arrow widths describe the magnitude of the path coefficients, and blue and red colors indicate for positive and negative effects, respectively. Path coefficients and coefficients of determination (R^2) were calculated after 999 bootstrap replicates and significance levels are indicated by * (P < 0.05), ** (P < 0.01) and *** (P < 0.001) levels. (b): Standardized effects (direct and indirect effects) derived from the partial least squares path models. (c): Variation partitioning analysis (VPA) comparing the effects of different composting properties including pH, NO_3^-, and WC on the ARGs abundances. The explanatory factor with values less than 0.01 (explained < 1% of total ARGs variations) was removed from VPA results. WC: water content, NO_3^--N: nitrate concentration. Relative abundance data was used to analyze PLS-PM.

724

725 **Table 1 Spearman's correlations between the relative abundance of ARGs and**

726 **MGEs during food waste composting**

727

Table 1 Spearman's correlations between the relative abundance of ARGs and MGEs during food waste composting

ARGs	Relative abundance of MGEs					
	intI1	*intI2*	*Tn916*	*ISR1*	*IncQ*	*Total MGEs*
tetA	0.414*	0.918**	0.885**	0.285	0.887**	0.901**
tetB	0.339	0.842**	0.888**	0.214	0.921**	0.888**
tetC	0.795**	0.554**	0.42*	0.589**	0.338	0.448*
tetG	0.797**	0.503*	0.645**	0.619**	0.55**	0.666**
tetL	0.204	0.643**	0.735**	0.055	0.806	0.73**
tetM	-0.296	0.17	0.341	-0.456*	0.517**	0.345
tetQ	0.807**	0.531**	0.432*	0.593**	0.344	0.465*
tetO	0.582**	0.69**	0.698**	0.255	0.675**	0.723**
tetW	0.505*	0.497*	0.659**	0.274	0.624**	0.675**
tetX	0.609**	0.558**	0.593**	0.456*	0.505**	0.59**
sul1	0.85**	0.561**	0.538**	0.651**	0.45*	0.572**
sul2	0.577**	0.884**	0.663**	0.51*	0.601**	0.705**
sul3	0.428*	0.823**	0.813**	0.376	0.781**	0.81**
strA	0.439*	0.77**	0.593**	0.289	0.529**	0.635**
strB	0.517**	0.744**	0.843**	0.37	0.815**	0.861**
aacA4	0.256	0.238	0.058	0.056	-0.034	0.090
aadA	0.453*	0.905**	0.771**	0.33	0.728**	0.808**
aadB	0.658**	0.53**	0.396	0.716**	0.227	0.429*
aadE	0.322	0.843**	0.846**	0.158	0.906**	0.843**
aphA1	0.237	0.147	-0.155	0.37	-0.154	-0.127
ermB	-0.269	-0.209	-0.283	-0.421*	-0.268	-0.268
ermF	0.497*	0.917**	0.871**	0.468*	0.812**	0.887**
ermM	0.11	0.492*	0.643**	-0.095	0.79**	0.62**
ermT	0.657**	0.579**	0.63**	0.524**	0.542**	0.663**
ermX	0.486*	0.035	-0.09	0.338	-0.215	-0.055
mefA	0.298	0.72**	0.677**	0.025	0.763**	0.682**
ereA	0.547**	0.61**	0.414*	0.261	0.44*	0.449*
Total ARGs	0.28	0.792**	0.895**	0.106	0.938**	0.904**

**Correlation is significant at the 0.01 level (2-tailed). *Correlation is significant at the 0.05 level (2-tailed).

Figure

Click here to download Figure: Figure-1201.docx

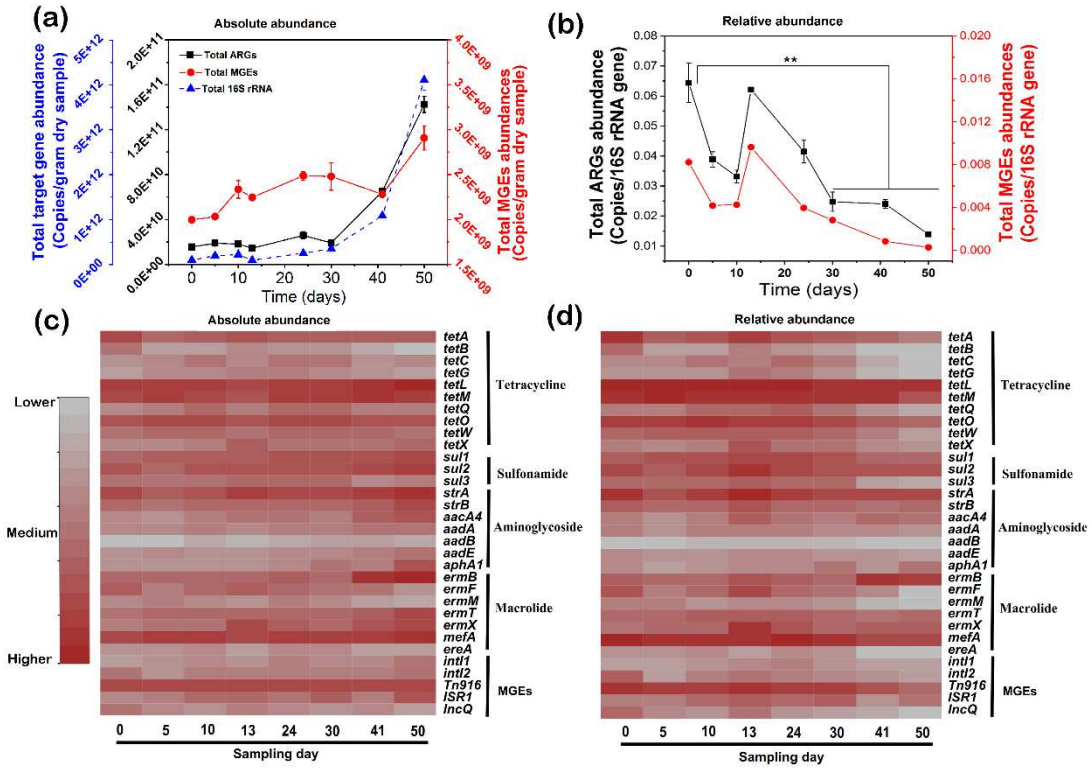

Figure 1

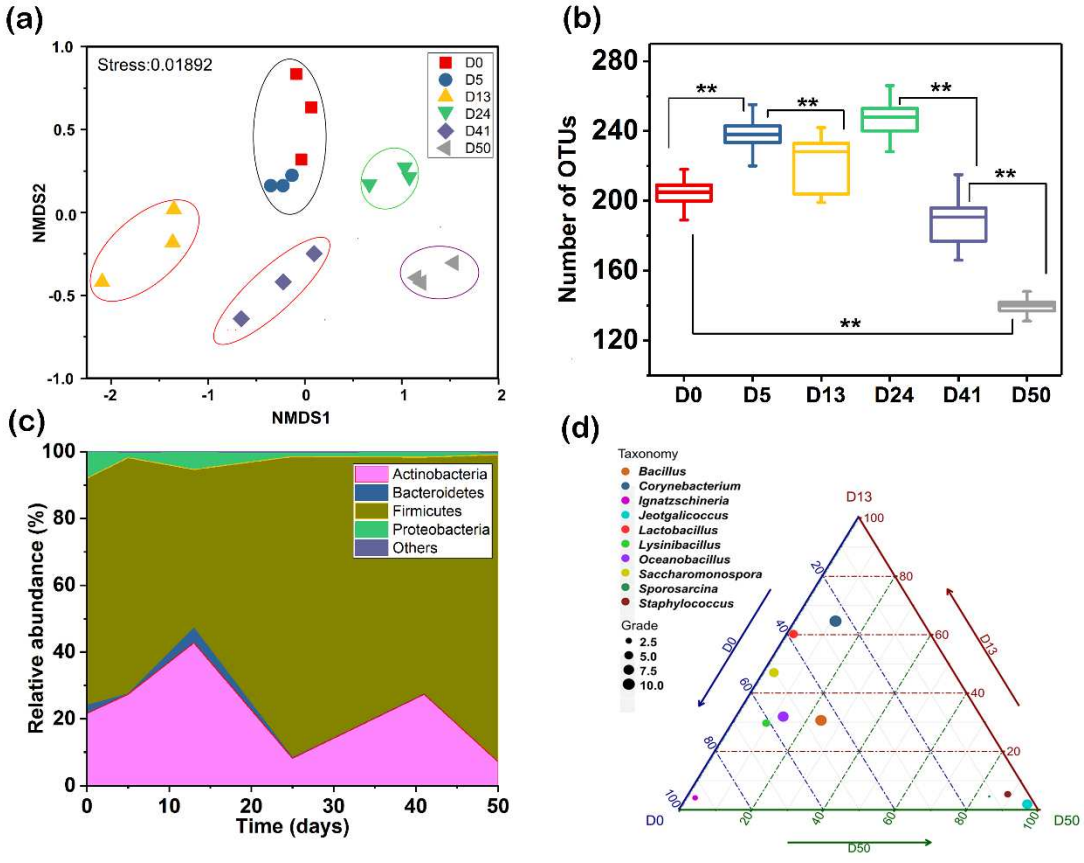
(a)
Stress:0.01892
D0
D5
D13
D24
D41
D50
NMDS2
NMDS1
(b)
Number of OTUs
**
D0
D5
D13
D24
D41
D50
(c)
Relative abundance (%)
Actinobacteria
Bacteroidetes
Firmicutes
Proteobacteria
Others
Time (days)
(d)
Taxonomy
Bacillus
Corynebacterium
Ignatzschineria
Jeotgalicoccus
Lactobacillus
Lysinibacillus
Oceanobacillus
Saccharomonospora
Sporosarcina
Staphylococcus
Grade
2.5
5.0
7.5
10.0
D0
D13
D50

Figure 2

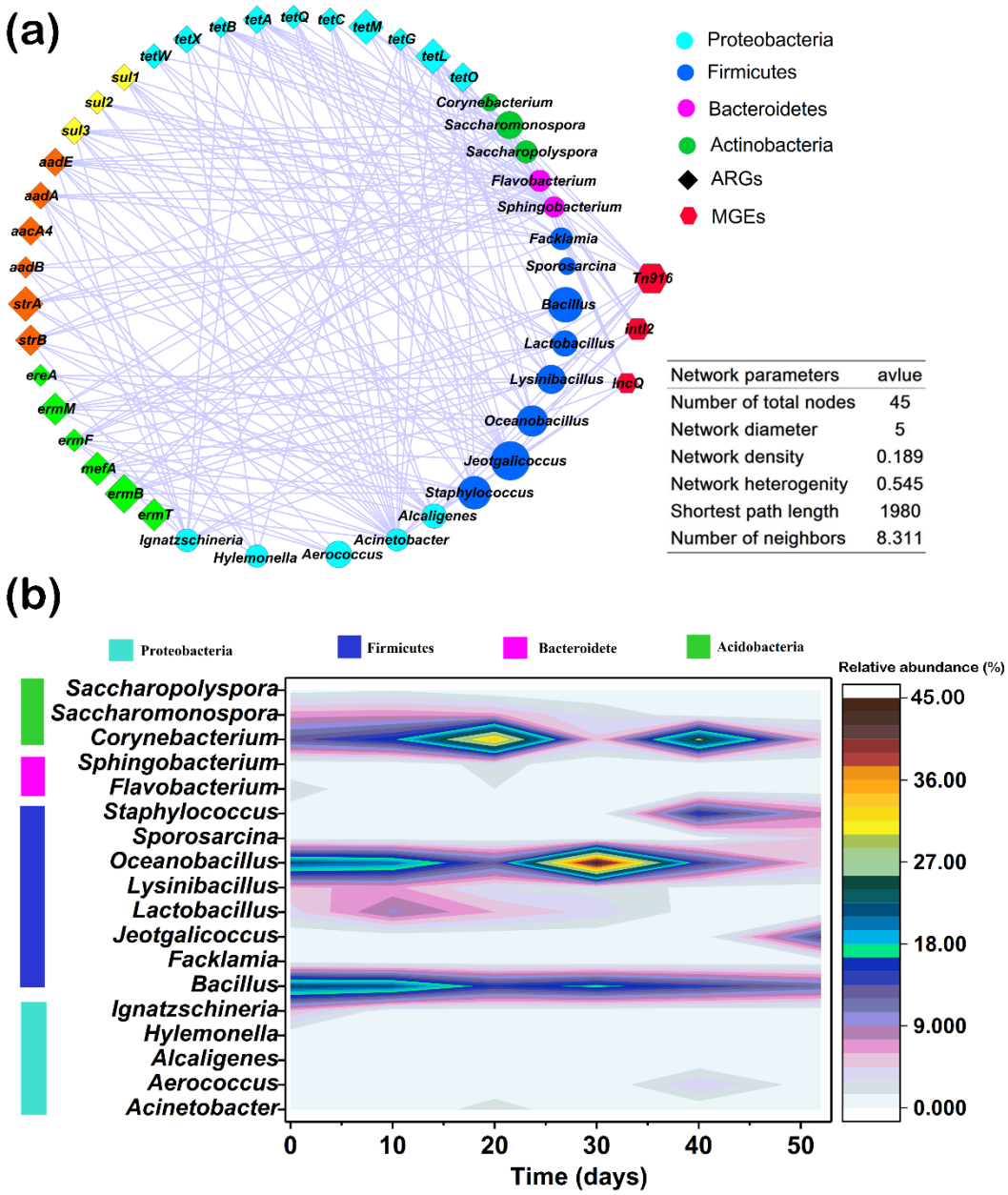
(a)
tetA
tetQ
tetC
tetM
tetG
tetL
tetO
tetB
tetX
tetW
sul1
sul2
sul3
aadE
aadA
aacA4
aadB
strA
strB
ereA
ermM
ermF
mefA
ermB
ermT
Corynebacterium
Saccharomonospora
Saccharopolyspora
Flavobacterium
Sphingobacterium
Facklamia
Sporosarcina
Tn916
Bacillus
intI2
Lactobacillus
Lysinibacillus
IncQ
Oceanobacillus
Jeotgalicoccus
Staphylococcus
Alcaligenes
Acinetobacter
Aerococcus
Hylemonella
Ignatzschineria
Proteobacteria
Firmicutes
Bacteroidetes
Actinobacteria
ARGs
MGEs
Network parameters avlue
Number of total nodes 45
Network diameter 5
Network density 0.189
Network heterogenity 0.545
Shortest path length 1980
Number of neighbors 8.311
(b)
Proteobacteria
Firmicutes
Bacteroidete
Acidobacteria
Relative abundance (%)
45.00
36.00
27.00
18.00
9.000
0.000
Saccharopolyspora
Saccharomonospora
Corynebacterium
Sphingobacterium
Flavobacterium
Staphylococcus
Sporosarcina
Oceanobacillus
Lysinibacillus
Lactobacillus
Jeotgalicoccus
Facklamia
Bacillus
Ignatzschineria
Hylemonella
Alcaligenes
Aerococcus
Acinetobacter
0
10
20
30
40
50
Time (days)

Figure 3

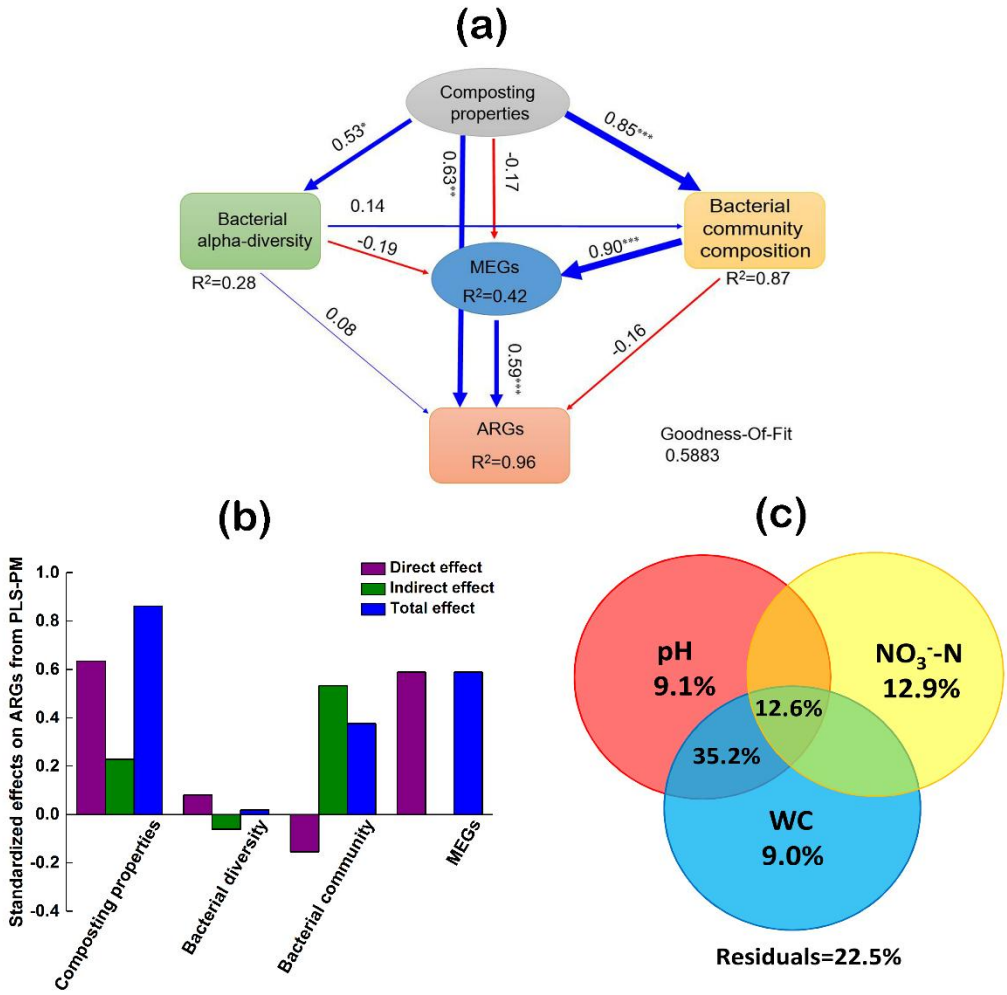
(a)
Composting properties
0.53*
0.85***
0.63**
-0.17
0.14
Bacterial alpha-diversity
Bacterial community composition
-0.19
0.90***
MEGs
R²=0.42
R²=0.28
R²=0.87
0.08
-0.16
0.59***
ARGs
R²=0.96
Goodness-Of-Fit
0.5883
(b)
Direct effect
Indirect effect
Total effect
Standardized effects on ARGs from PLS-PM
1.0
0.8
0.6
0.4
0.2
0.0
-0.2
-0.4
Composting properties
Bacterial diversity
Bacterial community
MEGs
(c)
pH
9.1%
NO3--N
12.9%
12.6%
35.2%
WC
9.0%
Residuals=22.5%

Figure 4

Supplementary material for on-line publication only

Click here to download Supplementary material for on-line publication only: Supplementary files_1201.docx